analytical chemistry

Article

pubs.acs.org/ac

High Sensitivity Detection and Quantitation of DNA Copy Number and Single Nucleotide Variants with Single Color Droplet Digital PCR

Laura Miotke,[‡,†] Billy T. Lau,[‡,§,†] Rowza T. Rumma,[‡,†] and Hanlee P. Ji*[,‡,§]

[‡]Division of Oncology, Department of Medicine, Stanford University School of Medicine, CCSR 1115, 269 Campus Drive, Stanford, California, 94305 United States

[§]Stanford Genome Technology Center, Stanford University, Palo Alto, California, 94304 United States

Supporting Information

ABSTRACT: In this study, we present a highly customizable method for quantifying copy number and point mutations utilizing a single-color, droplet digital PCR platform. Droplet digital polymerase chain reaction (ddPCR) is rapidly replacing real-time quantitative PCR (qRT-PCR) as an efficient method of independent DNA quantification. Compared to quantative PCR, ddPCR eliminates the needs for traditional standards; instead, it measures target and reference DNA within the same well. The applications for ddPCR are widespread including targeted quantitation of genetic aberrations, which is commonly achieved with a two-color fluorescent oligonucleotide probe (TaqMan) design. However, the overall cost and need for optimization can be greatly reduced with an alternative method of distinguishing between target and reference products using the nonspecific DNA binding properties of EvaGreen (EG) dye. By manipulating the length of the target and reference amplicons, we can distinguish between their fluorescent signals and quantify each independently. We demonstrate the effectiveness of this method by examining copy number in the proto-oncogene *FLT3* and the common V600E point mutation in *BRAF*. Using a series of well-characterized control samples and cancer cell lines, we confirmed the accuracy of our method in quantifying mutation percentage and integer value copy number changes. As another novel feature, our assay was able to detect a mutation comprising less than 1% of an otherwise wild-type sample, as well as copy number changes from cancers even in the context of significant dilution with normal DNA. This flexible and cost-effective method of independent DNA quantification proves to be a robust alternative to the commercialized TaqMan assay.

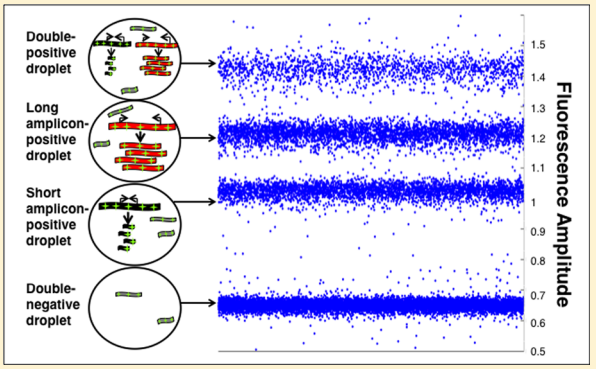

Digital PCR is a nucleic acid amplification and detection method that is based on the dilution of template DNA into independent noninteracting partitions.[1] Following Poisson statistics with high dilutions of DNA template, each reaction is independently interrogated for the presence of a nucleic acid at single molecule sensitivity. Digital PCR was first implemented on high dilutions of template DNA into microtiter plates[2] but has recently matured through the use of microfabricated platforms.[3−9] In recent years, several companies have produced commercially accessible ways to automate and expand the range of partitioning. This includes droplet digital polymerase chain reaction (ddPCR) systems (e.g., Bio-Rad QX200) that disperse template DNA randomly into emulsion droplets of equal volume.[9]

Recently, digital PCR has seen wider use as an analytical tool for research and clinical applications. For example, digital PCR can be used to detect mutations, to analyze copy number variations seen in the amplifications or deletions of specific genes, and to quantify specific nucleic acids species. Digital PCR can be useful for identifying cancer genetic variation from tumors, especially in clinical samples that are mixtures between normal and tumor DNA.

Commonly, digital PCR platforms rely upon the use of fluorescently quenched oligonucleotide probes to hybridize to a region of interest. Upon PCR amplification, the 5′ exonuclease activity of the polymerase separates the fluorophore from the quencher and generates a fluorescent signal specific to the target. The fluorescence of these partitions can be individually measured after amplification in order to determine the presence or absence of template molecules. The use of different fluorescent dyes allows for the simultaneous normalization of one genomic DNA region of interest (ROI) against a reference amplicon in a single reaction.[9] However, the major limitation of using fluorescent oligonucleotide probes in digital copy number analysis is the scalability of synthesis and optimization for a large number of genes.

Recent studies have explored the application of DNA binding dyes such as EvaGreen (EG) for the quantitation of single amplicons in a digital PCR format.[8,10] The EG fluorophore is a nonspecific double-stranded DNA (dsDNA) binding dye.

Received: November 26, 2013
Accepted: January 31, 2014
Published: January 31, 2014

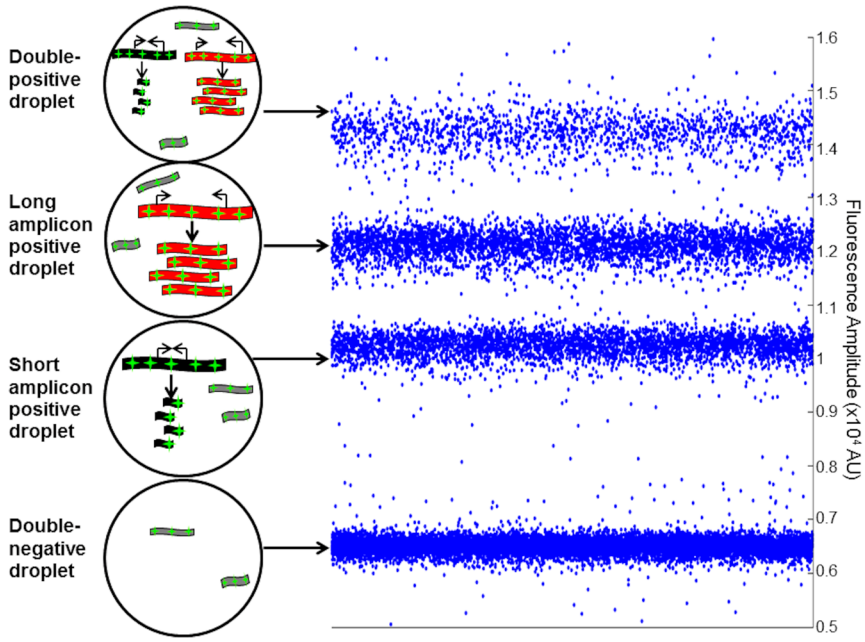

Figure 1. Schematic of droplet-digital PCR with EvaGreen dye. Droplets are formed pre-PCR by randomly sequestering fragmented template DNA into equal volume partitions. The first population of droplets corresponding with the lowest fluorescent amplitude has only the unamplified background template DNA (gray). The second population represents the droplets containing only the short amplicon template (black). For CNV analysis, this is UC1 (60bp), and for SNV analysis, this is the short-tail amplicon (71bp). The third population represents droplets with only the long amplicon template (red). For CNV analysis, this is the ROI (66bp), and for SNV analysis, this is the long-tail amplicon (104bp). The population with the highest amplitude represents droplets containing both amplified targets.

When no DNA is present, EG assumes an inactive low-background configuration; it only emits a strong fluorescent signal when DNA template is bound. The method of binding allows for the use of a higher concentration without inhibiting PCR and thus maintaining a higher resolution signal compared to SYBR dye.[11] The EG-DNA complex produces a maximum amplitude fluorescent signal at an excitation wavelength of 500 nm and an emission wavelength of 530 nm.[12] In comparison, digital PCR systems utilizing fluorescent oligonucleotide probes commonly consist of multiple spectrally distinct fluorophores for the detection of different targets. As only one wavelength can be used to detect both the reference and ROI in an EG-based digital PCR format, new multiplexing strategies independent of spectral context are required.

To achieve a multiplexed format in a single-color system, we took advantage of the varying amplitudes of EG signal for different amplicons using a Bio-Rad QX-200 system (Bio-Rad, Hercules, CA). Our assay utilizes differences in amplicon length for quantitative measurement of multiplexed copy number variation (CNV) or single nucleotide variants (SNVs) in a single well. Namely, we designed the ROI variant specific amplicon to be slightly longer that the reference nonvariant sequence. The increase in length of the amplicon results in an increase in the base pairs of double-stranded DNA present in a positive droplet. Since the fluorescent amplitude of the EG dye is proportional to the amount of dsDNA present, a droplet with a longer amplicon will fluoresce more brightly than a droplet with a shorter amplicon (Figure 1).

A correlation between amplified template length and droplet fluorescence amplitude has previously been reported in the context of TaqMan probe-based next-generation sequencing library characterization but not in the context of a single-color binding dye.[13] Recently, a study was published that demonstrated an EG-based droplet digital PCR platform as well as a proof-of-concept multiplexing approach based on amplicon length with the QX200 system.[14] In this work, we further expand this strategy to robustly detect and quantify CNVs across a wide range of targets and sample sources. We not only show that EvaGreen fluorescence amplitude varies based on amplicon length (Figure 2) but go on to manipulate this feature to multiplex two targets in one well. In addition, we extend this technique by direct manipulation of amplicon length in order to detect SNVs from cancer cell lines and patient samples. In both of our demonstrated CNV and SNV quantification strategies, we achieve high sensitivity and specificity, even in the context of genetic mixtures where the genetic variant of interest is represented only by a small fraction of the overall DNA.

EXPERIMENTAL SECTION

Ethics Statement. Sample DNA was collected from the Stanford Tissue Bank and approved by the Institutional Review Board (IRB) of Stanford University School of Medicine.

DNA Samples and Processing. We used human genomic DNA as the template in all digital PCR assays in this study. The control DNA was sourced from a Yoruban individual (NA18507; Coriell Institute, Camden, NJ). We obtained genomic DNA (NA18507, NA04626, NA06061) with varying degrees of X-chromosome aneuploidy from the Coriell Institute. Patient samples were sourced from colorectal tumor-normal pairs from the Stanford Cancer Institute Tissue Bank. We processed these tumor samples with the E.Z.N.A DNA/RNA/Protein extraction kit (Omega Bio-Tek, Norcross, GA) and treated post extraction samples with RNase A for 1 h at 37 °C. All *FLT3*-amplified colorectal cell lines were extracted from culture using the DNeasy Tissue Kit (Qiagen, Hilden, Germany) following the manufacturer's protocols. Cancer cell line DNA (LS411N, NCIH716, HT29) was obtained from ATCC (Manassas, VA) and Dr. Walter Bodmer (Cambridge, UK).

dx.doi.org/10.1021/ac403843j | *Anal. Chem.* 2014, 86, 2618−2624

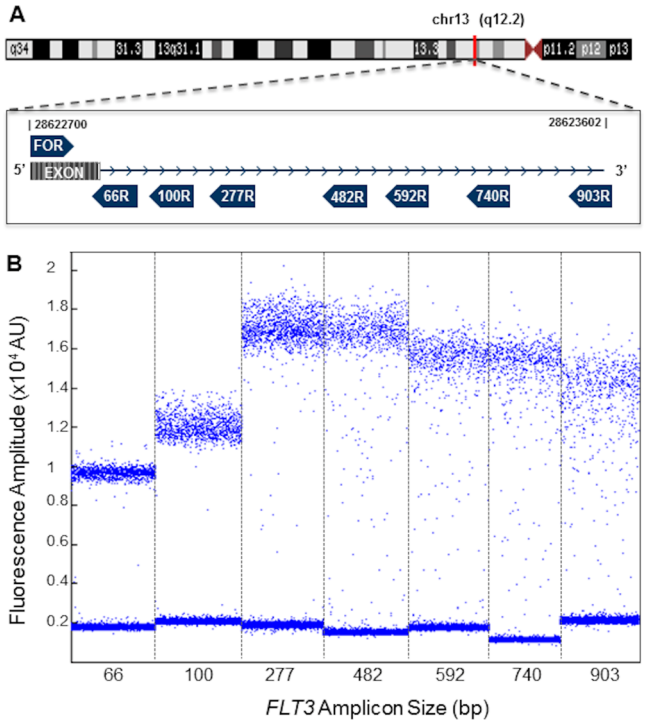

Figure 2. Correlated increase in amplicon length and EvaGreen fluorescence amplitude. (A) Reverse primers were designed to flank increasing length regions of *FLT3* with a common forward primer. All primers were approximately 20 bp. (B) Each column represents individual wells of ~20,000 droplets with a single set of *FLT3* primers. Amplicons >500 bp were allowed to anneal/extend for two minutes instead of one.

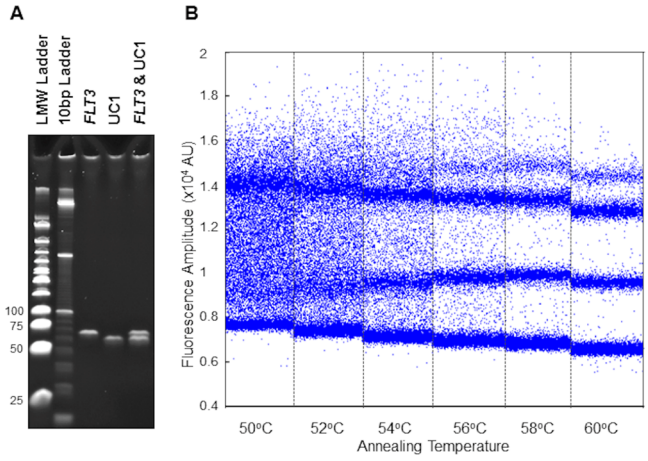

Figure 3. Primer optimization for CNV assay. (A) NA18507 normal diploid genomic DNA served as template for simplex PCR amplification of *FLT3* (66bp), UC1 (60bp), and a multiplexed reaction for both targets. Amplicons were run on a nondenaturing TBE acrylamide gel. (B) Each column represents a single well of ~20,000 droplets containing NA18507 template with multiplexed UC1 and *FLT3*.

Primer Design and Optimization. For all copy number assays, we designed primers to be around 20 bps in length using Primer3, verified their specificity with UCSC Genome Browser Primer BLAT, and purchased them from IDT (Integrated DNA Technologies, Coralville, IA). Primer sequences are listed in Table 1. For each, we performed simplex PCR using human genomic control DNA, NA18507 (Coriell), and confirmed the presence of the correct products with electrophoresis on a nondenaturing TBE acrylamide gel (Figure 3A). For all mutation quantification assays, we designed primers and verified specificity using IDT's PrimerQuest (http://www.idtdna.com/Primerquest/Home/Index). We designed the region of primers to be around 20 bps in length with the SNP as the last base pair on the 3′ end and melting temperatures within 3 °C of each other. Using NA18507 and LS411N (ATCC), we confirmed the presence of specific bands on a 2% agarose gel and then designed noncomplementary tail sequences of varying lengths to be added to the 5′ end. Short tails had high GC content, while long tails were AT rich to maintain melting temperatures within 3 °C of each other.

ddPCR Assay Conditions and Optimization. As the initial step, we treated all of the genomic DNA samples with the restriction enzyme EcoRI for 1−2 h at 37 °C, with subsequent heat-kill at 65 °C for 20 min. This restriction enzyme digest ensured that all potentially linked tandem gene copies in our high-quality DNA would be randomly and independently distributed into the droplets.

For all assembled 20 μL PCR reaction mixtures, we included 2× EvaGreen ddPCR Supermix (Bio-Rad) and primers at a final concentration of 0.1 μM. We loaded 20 ng of NA18507 template

Table 1. Primer Sequences

gene	length (bp)	forward	reverse
UC1	60	TGAGGGATTCGGCAGATGTTG	CTGAAAGGCTGGACTTGACAGA
FLT3	66	GGGATAGGACTCCTGGGTTT	GTGAGCAGCCTGCATTACCT
FLT3[a]	66	TCAGTGGCAAGAAACGACAC	AGCTGATTGACTGGGATGCT
FLT3	100	TCAGTGGCAAGAAACGACAC	GTGAGCAGCCTGCATTACCT
FLT3	277	TCAGTGGCAAGAAACGACAC	ATTCAAGCGAGCCTGGTTTA
FLT3	482	TCAGTGGCAAGAAACGACAC	CAGTGCTCACTGCCCTAACA
FLT3	592	TCAGTGGCAAGAAACGACAC	CATTATGGCTGAACGCTGTG
FLT3	740	TCAGTGGCAAGAAACGACAC	CAGCACCACTCTTCCATTGAT
FLT3	903	TCAGTGGCAAGAAACGACAC	CTGCAGGTCAGGTTGGATAAT
G6PD	64	GCCAGTGGCAGAGTAAGGAG	TCTCCTGGGTCTCAGGCTTA
BRAF-WT	65	CATGAAGACCTCACAGTAAA	CCACTCCATCGAGATTTCA
BRAF-MUT	65	CATGAAGACCTCACAGTAAA	CCACTCCATCGAGATTTCT
long tail	39		AAATAAATAAATAAATAAATAAATAAATAAATAAA
short tail	6		GGGGGG
forward tail	6	GGGGGG	

[a]Used for amplicon length experiment.

dx.doi.org/10.1021/ac403843j | *Anal. Chem.* 2014, 86, 2618−2624

DNA into all reactions with the exception of assays examining fluorescence intensity as a function of the amount of template DNA. We partitioned each reaction mixture into approximately 20,000 droplets with a droplet generator (Bio-Rad QX-200) and then cycled with the following conditions: 95 °C for 5 min (1 cycle); 95 °C for 30 s and 52−62 °C for 1 min (40 cycles); 4 °C for 5 min, 90 °C for 5 min (1 cycle), 4 °C hold. Cycled droplets were read individually with the QX200 droplet-reader (Bio-Rad).

For optimization of new primer sets, we used an annealing temperature gradient for PCR. On the basis of this assessment, we chose an annealing temperature of 60 °C for the *FLT3* primers and 61 °C for *G6PD* primers in the CNV assays. For SNV primers, we first ran one annealing temperature gradient for tailless primers. Subsequently, we employed a temperature gradient for primers with tails using a segmented annealing step as follows: 95 °C for 30 s and the optimal annealing temperature for tailless primers for 1 min (4 cycles); 95 °C for 30 s and 52−62 °C for 1 min (41 cycles). For the *BRAF* V600E primers, we used an annealing temperature of 55 °C for 4 cycles and then ramped up to an annealing temperature of 60 °C for 41 cycles.

Clustering Analysis of Droplet PCR. We exported the fluorescence amplitude of each droplet from the QuantaSoft droplet reader software (Bio-Rad) and, briefly, clustered the droplets into distinct groups using a distance-based minimum-variance linkage algorithm in MATLAB (Mathworks, Natick, MA). We eliminated droplets with extreme outlying amplitudes (<0.01% of the total droplets) from the analysis pipeline. We computed the number of negative droplets as if all droplets from three replicate wells were pooled together into one well. The concentration of each target was calculated as follows:

$$\frac{-\ln\left(\frac{\text{negative droplets}}{\text{total droplets}}\right)}{\text{droplet volume}} \quad (1)$$

Droplets intermediate between two cluster populations did not significantly alter the calculated concentration.

For copy number reactions run without replicates, we clustered the droplets and calculated copy number using the QuantaSoft software. The error reported for a single well was the Poisson 95% confidence interval. We used the automated clustering analysis for both *FLT3* and *G6PD*. We calculated copy number as 2× the ratio of ROI concentration versus reference concentration. We calculated the average and standard deviation across triplicates as weighted by the number of detected droplets in each well.

We used the automated clustering analysis for *BRAF* mutation quantification as described above. Percent mutant was calculated as follows:

$$\left(\frac{[\text{MUT}]}{[\text{MUT}] + [\text{WT}]}\right) \times 100 \quad (2)$$

We calculated the average and standard deviation across triplicates as weighted by the number of detected droplets in each well.

Amplicon Length Experiment. We used the cycling protocol described above; except for longer amplicons (>500 bp), we extended the annealing/extension step to 2 min. For this assay we ran only one well per template amount and generated copy numbers and 95% Poisson confidence intervals with the QuantaSoft platform.

Amplified DNA Spike-in Experiments. We used the cycling protocol for CNV as described above. We reported the copy number for NCIH716 from Cancer Cell Line Encyclopedia microarray data[15] and from Coriell Institute for NA18507. Dilutions of 1:5, 2:3, 3:2, and 5:1 of NCIH716 to 18507 DNA were made by volume using DNA samples that were equimolar.

Quantitative SNV Measurements on Controls and Spike-in Experiments. All expected mutation concentrations from cancer cell lines and control human DNA were derived from ddPCR with the PrimePCR *BRAF* V600E TaqMan assay (Bio-Rad). For these TaqMan control assays, we cycled with a single annealing temperature of 55 °C as per manufacturer recommendation. Concentration of mutant was calculated from triplicate using the Bio-Rad QuantaSoft platform. Subsequently, we used the concentrations (copies/ul) derived from the TaqMan assay to create dilutions of LS411N DNA into wild-type Human Male Control (Invitrogen, Carlsbad, CA). We analyzed dilutions of 40%, 30%, 20%, 5%, 1%, and 0.5% of mutant copies into wild-type. This assay relied on the same cycling protocol for EG mutation quantification as described previously.

RESULTS AND DISCUSSION

We developed single color ddPCR assays to measure two classes of genetic variation: (1) copy number variations and (2) SNVs. As a proof-of-principle, we designed assays to quantify the copy number amplification of the oncogene *FLT3* and the *BRAF* V600E mutation, frequent in colon cancer and melanoma. To develop these assays, we conducted a number of pilot optimization experiments.

The ability to multiplex two genes in a single-color ddPCR system is contingent on the ability to distinguish between double negative, single positive, and double positive droplet clusters (Figure 1). Differences in the fluorescence amplitude, determined by the amount of EG dye bound, can be used to distinguish these droplet populations. We show that, in a singleplex ddPCR reaction, the amplicon length can be used to manipulate the fluorescence of a particular droplet.

When we increased the amplified length of a *FLT3* region, we saw a correlation in increasing fluorescence amplitude with increasing amplicon size up to 500 bp (Figure 2). With amplicons longer than 500 bp, there was a decrease in positive-droplet fluorescence and an increase in the number of droplets with intermediate fluorescence. This phenomenon implies that amplification of these long regions may be incomplete.

Copy Number Determination. On the basis of this assessment, we designed a reference target and ROI with differing amplicon lengths in order to assess copy number. We verified the presence of the two correctly sized PCR products by electrophoresis on a nondenaturing acrylamide gel (Figure 3A). Additionally, we were able to identify four distinct droplet populations corresponding to the presence of one or both of the amplicons (Figure 3B). We found that across a range of annealing temperatures, 60 °C produced the most distinct droplet population separation for the *FLT3*-UC1 gene pair. The disparity in droplet population across temperatures indicates that the multiplexed nature of this assay is largely dependent upon the amplification efficiency of the ddPCR reaction. This aspect must be considered when designing primers to multiplex in an EG ddPCR system.

The amount of starting template DNA added per reaction can also affect the degree of droplet population separation. Due to the nonspecific binding fluorescence of the EG dye, the

dx.doi.org/10.1021/ac403843j | *Anal. Chem.* 2014, 86, 2618−2624

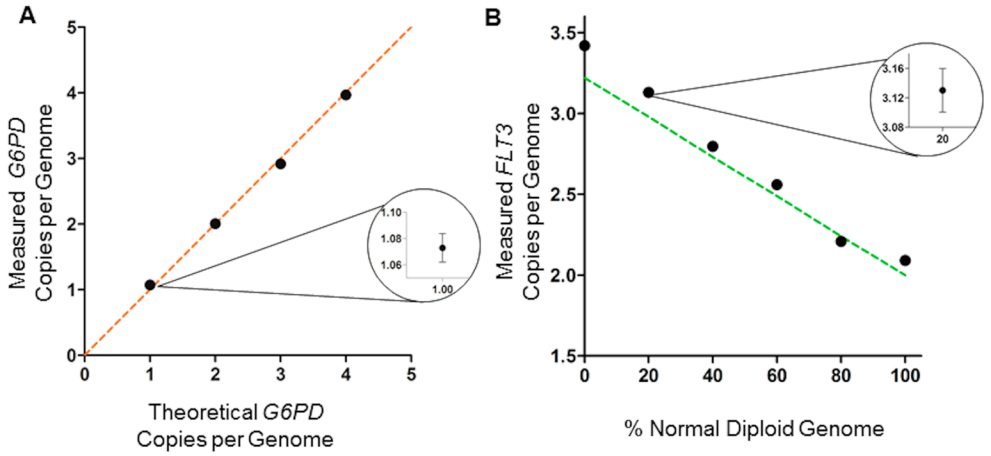

Figure 4. Sensitivity testing of EvaGreen CNV assay on control DNA. (A) G6PD copy number measured in four human X-chromosome disorder DNA samples (Coriell). The expected one-to-one line (orange) is based on the copy numbers provided by the Coriell Institute. (B) FLT3 copy number as measured in a serial dilution of NCIH716 colorectal cancer cell line into a normal diploid human control, NA18507 (Coriell). The expected copy number (green) was calculated from the Cancer Cell Line Encyclopedia (Broad) data on copy number derived from microarray analysis.

background signal of the unamplified product in the negative droplets increases with the amount of template DNA loaded. Also, the difference in fluorescence between negative and positive droplets accordingly shrinks. With starting template concentrations ranging from 0.25 to 2.5 ng/μL, we found that there was a clear amplitude separation between the droplet clusters (Figure S-1, Supporting Information). Although the populations were significantly condensed at higher concentrations, we were still able to accurately cluster droplets with a final DNA template concentration up to 10 ng/μL. Because the ROI and reference amplicons make up an extremely small fraction of the total human genome size, we are still in the Poisson dilution threshold for digital PCR. Additionally, we found that as little as 1 ng of high-quality DNA (NA18507) in a 20 μL reaction was required to yield an expected copy number close to two (Table S-1, Supporting Information).

Regardless of the concentration of initial template, our human control DNA sample had a *FLT3* copy number reproducibly close to two. This is the expected result for a normal diploid genome, reflective of a one-to-one ratio between the number of *FLT3* positive droplets and UC1 positive droplets (Figure S-1, Supporting Information). When choosing a reference gene, we wanted to confirm that disparities in primer efficiency between UC1 and *FLT3* did not significantly contribute to fluorescent amplitude. If the primer efficiency is not the same, we might expect that a less efficient primer pair would produce lower amplitude droplets (Figure S-2, Supporting Information). In that case, we would also expect the number of positive droplets in the lower amplitude population to be less. However, because there was no difference in the number of UC1 positive droplets versus *FLT3* positive droplets, we are confident that primer efficiency does not play a major role in determining fluorescent amplitude in our assay.

We explored the accuracy of our assay in detecting integer level CNV by analyzing the number of copies of the X-linked gene, *G6PD*, in DNA samples from patients with known X-chromosome aneuploidy. We accurately distinguished between *G6PD* copy numbers ranging from 1 to 4 at close to integer values (Figure 4A). This indicates the ability of the assay to not only evaluate copy number amplification but also offer an accurate metric for detecting gene deletions. The standard deviations of copy numbers detected varied in the one hundredth to thousandth of a copy, indicating a highly reproducible method with research and diagnostic potential to detect germline CNV.

While all of our DNA samples yielded near integer copy number values, this is not always the case in cancer samples (Table S-2, Supporting Information). Most clinical tumor samples are a mixture of normal and tumor cells at varying percentages, as well as genetically dissimilar subclones of cancer cells. To assess the sensitivity of our system in detecting heterogeneous tumor samples, we measure *FLT3* copy number in an amplified cell line (NCIH716) diluted into normal diploid DNA (NA18507). NCIH716 has a tumor cell line, a *FLT3* amplified copy number of around 3.5 copies per genome. We found that our method had the sensitivity to detect a tumor sample diluted 1:4 in normal template (Figure 4B). The performance of the assay on mixed samples indicates robust copy number evaluation in cancer samples that are tumor and normal cell mixtures.

Quantitative Detection of Single Nucleotide Variants. In addition to copy number assessment, we designed an assay for the *BRAF* V600E point mutation using the same concept of amplicon length variation to separate droplet populations. The design incorporated a long, noncomplementary tail onto the 5′ end of the *BRAF* wild-type primer and a short tail onto the BRAF mutant primer. The longer amplicon produced higher amplitude positive droplets than the shorter amplicon; thus, the population of wild-type positive droplets and mutant positive droplets were distinctly clustered and quantified similar to the CNV assay (Figure 5A).

We tested this primer mix on a series of diploid control DNA, cancer cell lines, and a colorectal patient sample for which next-generation sequencing had verified the presence of the targeted mutation. In all cases, we compared our method of multiplexing with EG to BioRad's commercially available PrimePCR *BRAF* V600E assay, which utilizes TaqMan chemistry. In BioRad's assay, a FAM probe hybridizes to the mutant sequence and a HEX probe hybridizes to the wild-type sequence, so each are read as separate clusters on two distinct channels. The EG reported values were similar to the values generated from Bio-Rad's commercially available PrimePCR *BRAF* V600E assay, which utilizes TaqMan chemistry. The concentrations (copies/μL) of mutant and wild-type measured with PrimePCR for each of the

dx.doi.org/10.1021/ac403843j | *Anal. Chem.* 2014, 86, 2618−2624

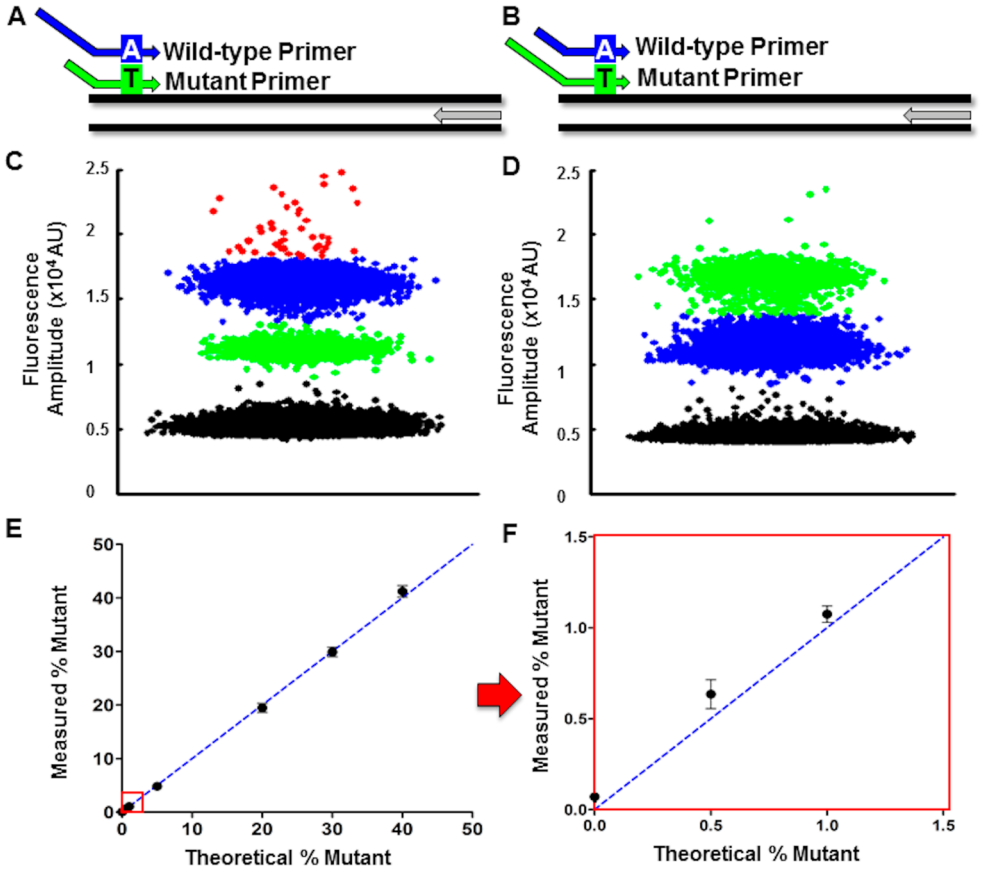

Figure 5. One-color SNV quantification. (A) Primers are designed with the single nucleotide variant at the 3′ end of the complementary region. Noncomplementary tails of varying lengths are then added to the 5′ end and amplified with a universal reverse primer. (B) 1:4 mixture of MUT/WT *BRAF* template amplified with mutant primers with the short tail and wild-type primers with the long tail. (C) Swap: 1:4 mixture of MUT/WT *BRAF* template amplified with wild-type primers with the short tail and mutant primers with the long tail. (D) Serial dilution of mutant *BRAF* template (LS411N) into wild-type (Human male control). Theoretical % mutant was calculated from TaqMan measured concentrations of mutant and wild-type template. The assay was performed with the EvaGreen primer mix from (B). (E) The red border regions provide a magnified view of three data points on the lower end of the dilution series from (D).

Table 2. Comparison between EvaGreen and TaqMan Mutation Quantification Methods on Control Template DNA

		% mutant	
template	source	Evagreen	TaqMan
18507	normal diploid DNA	0.01	0.00
Human Male Control	normal diploid DNA	0.00	0.00
HT29	cancer cell line	25.38	25.68
LS411N	cancer cell line	67.48	66.36
168B	patient-benign	0.00	0.00
168M	patient-malignant	25.30	27.13

control samples were used as a reference throughout our study. The EG measured values for the controls were universally similar to these reference values (Table 2).

To further test the accuracy of our assay in comparison to its TaqMan counterpart, we used our *BRAF* tail assay to amplify a known template mixture (80% wild-type template and 20% mutant template). Three populations were easily distinguishable and we measured the ratio of mutant to wild-type as 0.24 (Figure 5B). Next, we engineered a "swap" so that the wild-type primer was designed with the short tail and the mutant primer with the long tail. Using the same template mixture (4:1), we measured the ratio of wild-type template to mutant as 0.26 (Figure 5C). The close correspondence of these results to the genotype representation indicates amplicon length as the primary factor in determining population amplitude.

Finally, we measured the sensitivity of our mutation detection assay by performing a dilution of mutation template into increasing amounts of wild-type genomic DNA lacking the mutation (Figure 5D). Even at an expected mutation concentration of less than 1%, the single color assay could accurately quantify the mutant (Figure 5E). This has implications for the use of this method in detecting rare nucleotide variants, as well as mutation detection in low concentration samples such as circulating nucleic acids.

CONCLUSION

We demonstrated the multiplexed quantification of nucleic acids in a one-color digital PCR format by exploiting the shift in fluorescence amplitude due to varying amplicon size. This method retains the accuracy found in TaqMan-based droplet digital PCR platforms while eliminating the need for optimization of the probe oligonucleotide. Sampling error is minimized because both the ROI and the reference gene are measured from the same template. We showed that this single-color ddPCR strategy is robust in analyzing germline copy number variations, as well as quantifying copy number variation in admixtures between tumor and normal DNA. Through the direct manipulation of amplicon size using 5′ primer tails,

dx.doi.org/10.1021/ac403843j | *Anal. Chem.* 2014, 86, 2618−2624

we were also able to detect and quantify single nucleotide mutations at very low concentrations.

Since a third oligonucleotide is unnecessary in this system, it is possible to use shorter amplicons, which is preferable in the context of degraded DNA. Whereas TaqMan-based assays are limited by the efficiency of the oligonucleotide probe and dependent on the neighboring nucleotide context, our single-color digital PCR strategy is a highly flexible platform that can be used to interrogate a wide range of genetic targets.

■ ASSOCIATED CONTENT

Supporting Information

Figures and tables describing the optimization of starting genomic DNA per reaction, the effect of primer efficiency on fluorescent amplitude, and colorectal cancer patient *FLT3* copy numbers. This material is available free of charge via the Internet at http://pubs.acs.org.

■ AUTHOR INFORMATION

Corresponding Author

*E-mail: genomics_ji@stanford.edu. Phone: 650-721-1503. Fax: 650-725-1420.

Author Contributions

†L.M., B.T.L., and R.T.R. contributed equally to this work.

Notes

The authors declare no competing financial interest.

■ ACKNOWLEDGMENTS

This work was supported by the following National Institutes of Health (NIH) grants: NHGRI P01 HG000205 (B.T.L., H.P.J.) and Digestive Disease Center DK56339 (H.P.J.). H.P.J. and L.M. were supported by a Research Scholar Grant, RSG-13-297-01-TBG from the American Cancer Society. H.P.J. was also supported by the Doris Duke Clinical Foundation Clinical Scientist Development Award, a Howard Hughes Medical Institute Early Career Grant, the Clayville Foundation, and the Don and Ruth Seiler Fund.

■ REFERENCES

(1) Sykes, P. J.; Neoh, S. H.; Brisco, M. J.; Hughes, E.; Condon, J.; Morley, A. A. *BioTechniques* **1992**, *13*, 444.

(2) Vogelstein, B.; Kinzler, K. W. *Proc. Natl. Acad. Sci. U.S.A.* **1999**, *96*, 9236.

(3) Ottesen, E. a.; Hong, J. W.; Quake, S. R.; Leadbetter, J. R. *Science (New York, N.Y.)* **2006**, *314*, 1464.

(4) Warren, L.; Bryder, D.; Weissman, I. L.; Quake, S. R. *Proc. Natl. Acad. Sci. U.S.A.* **2006**, *103*, 17807.

(5) Heyries, K. A.; Tropini, C.; VanInsberghe, M.; Doolin, C. *Nat. Methods* **2011**, *8*, 6.

(6) Kiss, M. M.; Ortoleva-Donnelly, L.; Beer, N. R.; Warner, J.; Bailey, C. G.; Colston, B. W.; Rothberg, J. M.; Link, D. R.; Leamon, J. H. *Anal. Chem.* **2008**, *80*, 8975.

(7) Beer, N. R.; Wheeler, E. K.; Lee-Houghton, L.; Watkins, N.; Nasarabadi, S.; Hebert, N.; Leung, P.; Arnold, D. W.; Bailey, C. G.; Colston, B. W. *Anal. Chem.* **2008**, *80*, 1854.

(8) Shen, F.; Du, W.; Kreutz, J. E.; Fok, A.; Ismagilov, R. F. *Lab Chip* **2010**, *10*, 2666.

(9) Hindson, B. J.; Ness, K. D.; Masquelier, D. a.; Belgrader, P.; Heredia, N. J.; Makarewicz, A. J.; Bright, I. J.; Lucero, M. Y.; Hiddessen, A. L.; Legler, T. C.; Kitano, T. K.; Hodel, M. R.; Petersen, J. F.; Wyatt, P. W.; Steenblock, E. R.; Shah, P. H.; Bousse, L. J.; Troup, C. B.; Mellen, J. C.; Wittmann, D. K.; Erndt, N. G.; Cauley, T. H.; Koehler, R. T.; So, A. P.; Dube, S.; Rose, K. a.; Montesclaros, L.; Wang, S.; Stumbo, D. P.; Hodges, S. P.; Romine, S.; Milanovich, F. P.; White, H. E.; Regan, J. F.; Karlin-Neumann, G. a.; Hindson, C. M.; Saxonov, S.; Colston, B. W. *Anal. Chem.* **2011**, *83*, 8604.

(10) Shen, F.; Sun, B.; Kreutz, J. E.; Davydova, E. K.; Du, W.; Reddy, P. L.; Joseph, L. J.; Ismagilov, R. F. *J. Am. Chem. Soc.* **2011**, *133*, 17705.

(11) Eischeid, A. C. *BMC Res. Notes* **2011**, *4*, 263.

(12) Mao, F.; Leung, W.-Y.; Xin, X. *BMC Biotechnol.* **2007**, *7*, 76.

(13) Laurie, M. T.; Bertout, J. A.; Taylor, S. D.; Burton, J. N.; Shendure, J. A.; Bielas, J. H. *BioTechniques* **2013**, *55*, 61.

(14) McDermott, G. P.; Do, D.; Litterst, C. M.; Maar, D.; Hindson, C. M.; Steenblock, E. R.; Legler, T. C.; Jouvenot, Y.; Marrs, S. H.; Bemis, A.; Shah, P.; Wong, J.; Wang, S.; Sally, D.; Javier, L.; Dinio, T. A.; Han, C.; Brackbill, T. P.; Hodges, S. P.; Ling, Y.; Klitgord, N.; Carman, G. J.; Berman, J. R.; Koehler, R. T.; Hiddessen, A. L.; Walse, P.; Bousse, L. J.; Tzonev, S.; Hefner, E.; Hindson, B. J.; Cauly, T. H.; Hamby, K.; Patel, V. P.; Regan, J. F.; Wyatt, P. W.; Karlin-Neumann, G. A.; Stumbo, D. P.; Lowe, A. J. *Anal. Chem.* **2013**, *85*, 11619−11627.

(15) Barretina, J.; Caponigro, G.; Stransky, N.; Venkatesan, K.; Margolin, A. A.; Kim, S.; Wilson, C. J.; Lehar, J.; Kryukov, G. V.; Sonkin, D.; Reddy, A.; Liu, M.; Murray, L.; Berger, M. F.; Monahan, J. E.; Morais, P.; Meltzer, J.; Korejwa, A.; Jane-Valbuena, J.; Mapa, F. A.; Thibault, J.; Bric-Furlong, E.; Raman, P.; Shipway, A.; Engels, I. H.; Cheng, J.; Yu, G. K.; Yu, J.; Aspesi, P., Jr.; de Silva, M.; Jagtap, K.; Jones, M. D.; Wang, L.; Hatton, C.; Palescandolo, E.; Gupta, S.; Mahan, S.; Sougnez, C.; Onofrio, R. C.; Liefeld, T.; MacConaill, L.; Winckler, W.; Reich, M.; Li, N.; Mesirov, J. P.; Gabriel, S. B.; Getz, G.; Ardlie, K.; Chan, V.; Myer, V. E.; Weber, B. L.; Porter, J.; Warmuth, M.; Finan, P.; Harris, J. L.; Meyerson, M.; Golub, T. R.; Morrissey, M. P.; Sellers, W. R.; Schlegel, R.; Garraway, L. A. *Nature* **2012**, *483*, 603.